JJBS

Volume 17, Number 2,June 2024
ISSN 1995-6673
Pages 247 – 257
https://doi.org/10.54319/jjbs/170204

Jordan Journal of Biological Sciences

The Role of Artocarpin In Inhibiting Wnt/B-Catenin Signalling Pathway Through Its Binding to Tcf-4/B-Catenin Complex in H460-Derived Lung Cancer Stem Cells.

Nik Nurul Najihah Nik Mat Daud[1], Noor Azlina Abu Bakar[2,*], Abdi Wira Septama[3], Badrul Hisham Yahaya[4], Norashikin Zakaria[4], Noor Zafirah Ismail[5], and Hasni Arsad[5]

[1] Department of Biomedical Science,Faculty of Applied Science, Lincoln University College Main Campus,No.2, Jalan Stadium, SS7/15, Kelana Jaya, 47301, Petaling Jaya, Selangor; [2] Faculty of Medicine, Universiti Sultan Zainal Abidin, Jalan Sultan Mahmud 20400, Kuala Terengganu, Terengganu,Malaysia; [3] Research Center for Pharmaceutical Ingredients and Traditional Medicine, National Research and Innovation Agency (BRIN), Cibinong Science Center (CSC), Bogor, West Java 16911, Indonesia; [4] Regenerative Medicine Cluster, Advanced Medical and Dental Institute (AMDI), Universiti Sains Malaysia, Bertam, 13200 Kepala Batas, Pulau Pinang, Malaysia; [5] Laboratory of Biocrystallography and Structural Bioinformatics, Advanced Medical and Dental Institute (AMDI), Universiti Sains Malaysia, Bertam, 13200 Kepala Batas, Pulau Pinang, Malaysia

Received: May 30, 2023; Revised: August 29, 2023; Accepted: September 27, 2023

Abstract

The presence of cancer stem cells (CSCs) in lung cancer could contribute to cancer development and unsuccessful treatment. β-Catenin protein has been found to play a crucial role in cell survival. As artocarpin has been postulated to exert important antitumor properties, this research was conducted to elucidate the effect of artocarpin in the suppression of CSCs through modulating the β-Catenin signalling pathway. Using isolated CSCs from lung adenocarcinoma cell lines (H460), the potential of artocarpin in suppressing CSC was assessed using MTT assay. The stemness gene expression was analysed using real-time quantitative polymerase chain reaction; meanwhile, the assessment of artocarpin binding affinity against the β-Catenin active site was performed using docking analysis and validated with RT-qPCR. A 62.5% of lung $CD166^{+}CD44^{+}$ CSCs cells and 37.5% of lung $CD166^{-}CD44^{-}$ non-CSCs cells were identified in the H460 cell line. The results revealed that artocarpin exerted the highest cytotoxic value against lung $CD166^{+}CD44^{+}$ CSCs with an IC_{50} value of 5.07 µg/mL compared to $CD166^{-}CD44^{-}$ non-CSCs and H460 cells which were 8.67 µg/mL and 9.07 µg/mL, respectively. Additionally, the expression of stemness genes such as KLF4, SOX2, and NANOG was found to be significantly reduced ($P< 0.05$) in the treated lung CSCs with fold change (FC) values of 0.025, 0.104, 0.074, respectively in 10 µM artocarpin. The molecular docking analysis showed that artocarpin possessed the best-docked complexes with β-Catenin and WNT protein with high binding energy values (-7.04 kcal/mol and -14.91 kcal/mol), respectively compared to other WNT/β-Catenin inhibitors including isorhamnetin, fisetin, genistein, silibinin, catechin, luteolin, coumestrol and β-naphthoflavone. These findings support the inhibitory activity of artocarpin on lung CSCs with low WNT and β-Catenin gene expression levels and FC values (0.155, $P<0.01$ and 0.129, $P<0.05$) in 10 µM artocarpin compared to untreated cells, respectively. Therefore, based on this study, it is suggested that artocarpin has the potential to be developed as a therapeutic agent to inhibit stem cell regeneration in lung cancer via the WNT/β-Catenin signalling pathway through inhibition of TCF-4/β-Catenin complex formation.

Keywords*:* artocarpin, cancer stem cells, differentiation assay, molecular docking and stemness gene.

1. Introduction

Cancer recurrence or relapse is one of the major concerns in cancer therapy. It is estimated that around one-third of all cancer patients will experience a recurrence at some point after their initial treatment. The risk of recurrence varies depending on the type of cancer, the stage at diagnosis, and the type of treatment received. Nowadays, there are many major treatments for cancer management including surgery, cytotoxic chemotherapy, targeted therapy, radiation therapy, endocrine therapy, and immunotherapy. Despite the achievements made in treating cancers during the past decades, resistance to

* Corresponding author. e-mail: noorazlina@unisza.edu.my.

** **Abbreviations** : ADHL Alcohol Dehydrogenase-like; CD166 Cluster of differentiation 166; CD133 Cluster of differentiation 133; CD44 Cluster of differentiation 44; cDNA complementary DNA; CSCs Cancer Stem Cells; DACT3 Dishevelled Binding Antagonist of β-Catenin 3; EpCAM Epithelial Cell Adhesion Molecule; FACS Fluorescence-activated Cell Sorting; IC50 Half maximal inhibitory concentration; KLF4 Kruppel-like factor 4; NANOG NANOG homeobox protein; OCT3/4 Octamer-binding transcription factor 3/4; RT-qPCR reverse transcription-quantitative polymerase chain reaction; SOX2 SRY-box transcription factor 2; WNT Wingless-related integration site family

classical chemotherapeutic agents and novel targeted drugs continues to be a challenge. With decades of research on cancer recurrent, it was found due to the presence of a small subsets of cells resides within the tumour, which can self-renew and maintain the tumorigenic characteristics. These cells are known as cancer stem cells (CSCs). CSCs are cancer cells that can self-renew and give rise to heterogeneous cancer cell lineages that comprise *an* entire tumour (Khatami *et al*., 2020; Almajali *et al*., 2021). According to Jahanafrooz *et al.* (2020), various studies have consistently found that the signalling pathway of CSCs is a critical factor and plays a crucial role in disease progression. Although the presence of CSCs has been studied in detail in many solid tumours (Huang *et al*., 2020), insufficient attention has been paid to lung cancer cells, especially H460 cell lines. In addition, it is still unclear if CSCs are present in all or only specific cancer cells. This is due to the resilience of CSC markers and the underestimation of tumorigenic cell frequencies detected by the current available techniques. Thus, the present study sought to isolate CSCs from H460 cells and investigate the effect of artocarpin in suppressing the proliferation of CSCs in H460 cells as a model cell line for non-small cell lung cancer cells (NSCLC), as well as to investigate the mechanism of action that triggers the suppression through the WNT/β-Catenin degradation pathway.

Several CSCs regulators have been determined, and the findings provide understanding of how CSCs drive tumour homeostasis. In many cancer types, aberrant gene expression is highly related to tumour development, progression, and treatment resistance (Huang *et al*., 2020). The process that governs the pluripotency maintenance and plasticity of CSCs involves the regulation of multiple transcription factors such as octamer-binding transcription factor 3/4 (OCT3/4), Sry-related HMG box 2 (SOX2), Kruppel-like factor 4 (KLF4), NANOG, and c-MYC (Van Schaijik *et al*., 2018). Although these transcription factors play essential roles in controlling the activity of specific genes in embryonic stem cells (ESCs), particularly those associated with stem cell pluripotency, cell differentiation, and cellular reprogramming, regulations of its expressions lead to cancerous growth (Pouremamali *et al*. (2022). While the precise source of CSCs remains a topic of ongoing research, multiple studies have put forth several hypotheses regarding their origin. These hypotheses include the fusion of a normal stem cell with a transformed cell, the horizontal transfer of an oncogene from an apoptotic cell to a normal stem cell resulting in its transformation into a CSC, and the potential for stem cells residing in a tissue for repair purposes to transform into CSCs in response to an inflammatory microenvironment, triggered by the release of cytokines during infection and inflammation (Nimmakayala *et al*., 2019).

In addition, other intracellular activities, such as the WNT/β-Catenin signalling pathway, also regulate CSC phenotypes (Yang *et al*., 2020). Fundamentally, this cascade is responsible for embryonic development. However, dysregulation of this signalling and its interaction with other critical regulatory components, such as the TCF4/β-Catenin complex, leads to self-renewal, tumorigenesis or malignancies, and metastasis of CSCs (Zhan *et al*., 2017). Marked overexpression of β-Catenin and TCF-4 protein was recorded in the CSCs population compared to non-CSCs, while its inhibition was reported to attenuate CSCs metastasis in various cancer types (Makena *et al*., 2020). TCF-4 is an E-protein (E-box) involved in various developmental aspects (Forrest *et al*., 2014). For example, the TCF-4 protein plays a role in the maturation of cells to carry out specific functions, including regulating a variety of neural genes involved in early development, differentiation, intrinsic excitability, synapses, and survival (Chen *et al*., 2021). According to Hwang *et al*. (2020), TCF-4's involvement in cell survival, and induction of anti-apoptosis mechanisms suggested that TCF-4 may be a molecular target for CSC regeneration.

Among many potentially natural-derived anticancer agents, artocarpin is on the list. This compound's anticancer activity against lung cancer cells has been studied extensively (Mat Daud *et al*., 2021); however, the mechanism of how this compound inhibits tumour progression and stemness characteristic of CSCs remains unexplored. The advancement of molecular docking technology can provide insight into the interaction of this compound with the specifically targeted component (β-Catenin and WNT protein) of the signalling pathway. What are the possible consequences of the binding energy between artocarpin with both proteins β-Catenin and WNT obtained to the level of the oncogene expression? This study sets out to address this research gap, contribute to the knowledge of isolating CSCs from the parental H460 cell lines, and explain the possible regulatory mechanisms exerted by this compound on isolated cells, thereby elucidating its anticancer mechanisms.

2. Materials and methods

2.1. Cell lines

The human lung adenocarcinoma (H460) cell line was purchased from the American Type Culture Collection (ATCC, Manassas, VA, USA). The cells were routinely cultured and incubated at 37°C with 5% CO_2. The cells were grown in 75 cm^2 tissue culture flasks and collected with 0.25% trypsin-EDTA once they reached 80% confluence.

2.2. Chemicals and reagents

All cancer cell lines were cultured in RPMI-1640 medium containing 10% foetal bovine serum (FBS) and 1% penicillin/streptomycin (Gibco, Life Technologies, Foster City, CA, USA). The DMSO was purchased from Sigma-Aldrich in Munich, Germany. The antibodies used includes CD44-FITC (Clone: L178; Isotype: Mouse IgG1, κ), CD166-PE (Clone: 3A4; Isotype: Mouse IgG1, κ) (BD Biosciences, San Jose, CA, USA), and EpCAM–FITC (Clone: 158206; Isotype: Mouse IgG2B; Isotype: Mouse IgG1, κ) (R&D System, Minneapolis, MN, USA).

2.3. Preparation of artocarpin compound

The pure compound of artocarpin was generously provided by Septama and Panichayupakaranant who isolated the sample as mentioned in Septama and Panichayupakaranant, 2015. In this study, artocarpin compound was prepared as a stock solution by dissolving 500 µg into 1 mL of absolute DMSO. Then, 1000 µL of artocarpin compound was mixed with 1 µL of absolute DMSO and 999 µL of culture media to produce 2000 µL of test solution for each tube containing 0.1% DMSO. Prior to cell treatment, five concentrations (31.25, 15.63,

7.81, 3.91, 1.95 µg/mL) for each compound were prepared for cytotoxicity test meanwhile two concentrations of artocarpin (10µM and 100µM) were prepared for CSCs characterization assays and gene expression. The prepared concentrations were determined based on dose-response curves obtained from MTT assay in a preliminary study for artocarpin on the H460 cell line. For conducting the experiments, stock solutions of artocarpin were prepared by dissolving 500 µg of the compound in 1 mL DMSO and stored at -20°C. The final DMSO concentration in each well was kept between 0.1% and 0.11% for the treatment of cells throughout the experiments.

2.4. Isolation of CSCs phenotype

CSCs were isolated based on their specific surface markers using corresponding specific antibodies (Satar *et al.* (2018). In detail, the confluent (80%) lung cancer cells were detached using trypsin and washed with 2% FBS mixed with phosphate buffer solution (PBS). The antibodies which include CD44-FITC (Clone: L178; Isotype: Mouse IgG1, κ), CD166-PE (Clone: 3A4; Isotype: Mouse IgG1, κ) (BD Biosciences, San Jose, CA, USA), and EpCAM–FITC (Clone: 158206; Isotype: Mouse IgG2B; Isotype: Mouse IgG1, κ) (R&D System, Minneapolis, MN, USA) were then used to label all of the cell suspensions. Following that, cells were mixed in 90 µL of 2% FBS PBS, to which 10 µL of each antibody was added, and incubated for 30 minutes in the dark. The unbound antibodies were then washed with PBS. Each cell pellet received 500 µL of 2% FBS PBS, and the mixture was filtered through a 40 µm cell filter to ensure the formation of a single-cell suspension. Using a fluorescence-activated cell sorter (FACS Aria III, BD Biosciences), cancer stem cell markers CD166, CD44, and EpCAM expressions were examined and sorted (Masciale *et al*., 2019).

2.5. Co-Expression of CSCs Surface Markers in Lung Cancer Cells

Briefly, the H460 cells were detached by incubating with trypsin at 0.25% concentration (80% confluency) for 5 minutes, followed by washing with phosphate buffer solution (PBS) containing 2% of Foetal bovine serum (FBS). Then, the cells were labelled with only two antibody types: CD44-FITC and CD166-PE excluded EpCAM–FITC as they were not detected in the identification process. A 10 µL of each of the respective antibodies were added into cell suspension containing 90 µL of PBS and 2% of FBS. They were incubated for 30 minutes in the dark condition. The cell suspension was centrifuged to obtain the cells bound with antibody, while the remaining unbound antibody in the supernatant was discarded. Afterward, 500 µL of PBS containing 2% of FBS was added into each cell pellet and re-suspended before the filtration process using 40 µm cell filters to ensure that a single cell suspension was obtained.

2.6. The cytotoxic assay of artocarpin compound

A cultured H460, lung CSC and non-CSC in RPMI-1640 media with 10% v/v FBS, 1% v/v penicillin-streptomycin in 25 cm^2 T-flask (GIBCO, USA), humidified with 5% CO2 at 37°C were plated in a 96-well plate (5×10^3 cells/well) and incubated for 24 hours. Each well was then filled with the prepared artocarpin compound and a medium containing 0.1% DMSO. Following 48 hours of incubation, 20 µL of MTT reagent (5 mg/mL) was added and incubated for another four hours. Following observation through a microplate reader (Spectra 340, Tecan Magellan PRO, Molecular Device, Sunnyvale, CA) at 570 nm, the aspirated medium was replaced with 150 µL of absolute DMSO. The number of viable cells was determined by measuring the absorbance value. The inhibitory percentage was obtained by dividing the absorbance of the sample by the absorbance of the control. The untreated cell served as a negative control meanwhile, cisplatin-treated cells served as a positive control.

2.7. CSCs transcription factors expression

To investigate the expression of CSCs transcription factors, two-step quantitative reverse transcription polymerase chain reaction (RT-qPCR) analyses were employed. Briefly, using a RNeasy Plus Mini Kit (Qiagen), the total amount of RNA was extracted from the isolated cells. cDNA was synthesized from 250 ng/µL of total RNA by using the GoScript Reverse Transcription System (Promega, Woods Hollow Road Madison, USA) focusing on random primer and oligo (dT)15 primer. Assays-on-Demand primer/probe sets, and TaqMan Universal PCR Master Mix (Applied Biosystems) were utilized for the RT-qPCR reactions. Assays included the stem cell-related genes SOX2, KLF4, NANOG, OCT 3/4, DACT3 (β-Catenin), and the reference gene; GAPDH genes (Applied Biosystems) were used. The RT-qPCR reaction was conducted using the ABI StepOnePlusTM PCR System (Applied Biosystems, Foster City, USA) with the following thermal cycling conditions: 10 minutes at 95°C (holding stage), followed by 40 cycles of denaturation for 15 seconds at 95°C and annealing and extension steps for 1 minute at 60°C using a StepOnePlusTM Real-Time PCR System Thermal Cycling Block (Applied Biosystems). The comparative CT (ΔΔCT) method was utilized for quantification. In this study, untreated cells served as the control sample, while the GAPDH gene served as the endogenous control (Zakaria *et al.,* 2015).

2.8. Data extraction

The β-Catenin protein 3D structural file (PDB ID: 1JDH) was extracted from the protein data bank (PDB) (www.rcsb.org/pdb), while artocarpin structures molecules were analysed and depicted using ChemDraw Ultra V6.0. PyMOL viewer 1.5.4 was used for the interactive visualization and analysis of protein-ligand. ADME-T properties of artocarpin were predicted in-silico using the organic chemistry portal at http://www.organic-chemistry.org/prog. Molecular docking was conducted using AutoDock v4.24 on Windows 10 platform (64-bit) with Lenovo 120S-11IAP machine (Intel® Celeron® CPU N3350 @ 1.10 GHz, 4 GB memory) (Hassan *et al.,* 2021).

2.9. Inhibition analysis by docking

Docking analysis was done using AutoDock v4.24 by comparing the docking results with other known inhibitors of WNT/β-Catenin pathway (isorhamnetin, fisetin, genistein, silibinin, catechin, luteolin, coumestrol, and β-naphthoflavone) exhibited -6.50 to -5.22 kcal/mol (Iftikhar and Rashid, 2014), whereby polar hydrogen atoms have been added to the β-Catenin receptor protein. Rotatable ligand torsions permit flexible ligand docking, including

arbitrary flexible orientations and torsions for ligands. A 40 × 40 × 40 Å3 grid with 0.375 between each point was constructed around the protein receptor to ensure all residues were accessible in any zone for ligand binding. The number of docking runs has been set at 100, with a population of 150 starting out, 2.5 × 10^6 energy assessments, a total of 27,000 iterations, a mutation rate of 0.02, and a crossover rate of 0.80. AutoDock performed cluster analysis on initially docked conformations with a root mean square tolerance of 1.0 Å to obtain final docking data (Hassan *et al*., 2021; Abd Wahab and Ibrahim, 2022).

2.10. β-Catenin and WNT knockdown analysis

In mammalian cells, a scalable approach for detecting changes in gene expression following RNA was developed (Fleige *et al*., 2006). This technique describes how to transfect cells, collect total RNA, synthesize cDNA, run qPCR reactions with multiplexed TaqMan dual hydrolysis probes and interpret qPCR findings using relative quantification (Muraro *et al*., 2012). The relative knockdown of a set of β-Catenin and WNT genes against a target can be measured using this method. The protocol for doing RT-qPCR was outlined in the previous section on CSC transcription factors expression.

2.11. Statistical analysis

All data were expressed as the mean ± Standard Error Mean (SEM) of three independent experiments. MTT assay was statistically analysed using Graph Pad Prism® v6.01. Meanwhile, the expression of selected genes was analysed using an ABI StepOnePlus™ v2.3 Real-Time PCR machine (Applied Biosystems, Foster City, CA, USA). The RT-qPCR reaction was prepared using a Taqman® gene expression assay (Applied Biosystems). The comparison between artocarpin treatment group with the untreated group was performed using an unpaired t-test. *P* values of <0.05 were considered statistically significant for each test's n=3 sample size.

3. Results

3.1. Expression of cancer stem cell (CSCs) markers

Since the small population subtype of CSCs in lung cancer cell lines ranged across cell lines, specific markers, including CD166, CD44, and EpCAM, as CSCs markers in human lung cancer cell lines are required for the identification and isolation processes. In the identification process, the H460 cell exhibited 52.6% of CD166 expression and 13.8% of CD44 expression; meanwhile, 0% of EpCAM expression was observed. In this study, both surface markers of CD166 and CD44 excluding EpCAM, have been expressed with varying levels of expression in all H460 cell lines (Figure 1A). As depicted in Figure 1B, two markers' (CD166 and CD44) co-expression was examined in which 62.5% of the H460 cells were $CD166^+CD44^+$ mwanwhile $CD166^-CD44^-$ with the percentage of expression as 37.5% cells were identified as a non-CSC population.

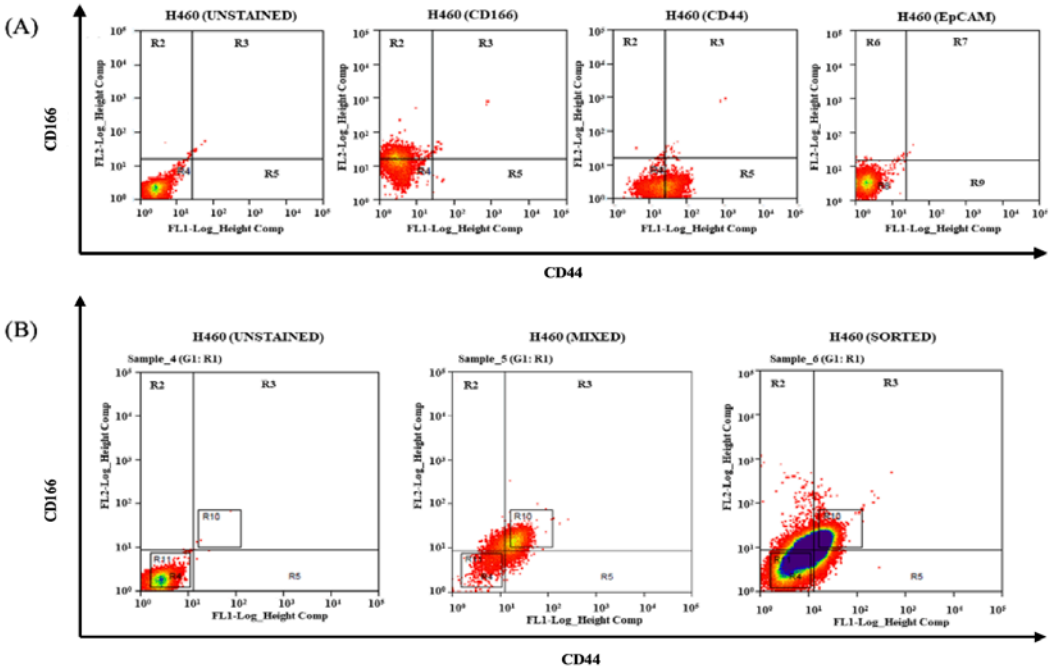

Figure 1. Flow cytometry analysis. (A) Identification of CD166, CD44, and EpCAM cells in H460 cancer cell line and (B) identification of co-expression of CD166/CD44 in H460 cancer cell lines. The cells were stained with anti-CD166 PE and anti-CD44 FITC.

3.2. Artocarpin cytotoxic assay on cancer cells line

The cytotoxic effect of artocarpin on cancer cells and cancer stem cells was demonstrated by the reduction in the number of living cells observed in the MTT assay. Artocarpin demonstrated an inhibitory impact on all cancer cell lines, as shown in Table 1. A significant difference was seen in each concentration (P<0.05) compared to control drug cisplatin. According to the result, a significant cytotoxic effect of artocarpin was observed against lung CSCs $CD166^+CD44^+$ followed by lung CSCs $CD166^-CD44^-$ (non-CSC) and H460 with IC_{50} values of 5.07±0.12, 8.67±0.10, and 9.07±0.24 µg/mL, respectively.

Table 1. Inhibitory concentration (IC_{50}) of artocarpin and cisplatin against parental H460 and lung CSCs

Cells Types	Artocarpin IC_{50} (µg/mL) ± SEM	Cisplatin IC_{50} (µg/mL) ± SEM
Lung CSC $CD166^+/CD44^+$	5.07 ± 0.12*	9.16 ± 0.05
Lung Non-CSC $CD166^-/CD44^-$	8.67 ± 0.10*	10.29 ± 0.05
H460	9.07 ± 0.24*	14.16 ± 0.19

Each data in the column represents the mean ± Standard Error Mean (SEM) with n=3. Unpaired t-test was used and the asterisk (*) indicates the significant difference of the compounds compared to cisplatin in each cell with P < 0.05.

3.3. Attenuation of stemness genes expression upon artocarpin treatment

All cell lines demonstrated detectable levels of the stem cell-related genes expression (Figure 2) except OCT 3/4. The KLF4, SOX2, and NANOG genes observed to be down-regulated with fold change (FC) values of 0.383 (P<0.001), 0.550 (P<0.001), and 0.338 (P<0.001), respectively in 10 µM of artocarpin treatment compared to their expression in the untreated cells. Further down-regulation was shown when using a higher dose of artocarpin (100 µM) with FC values of 0.055 (P<0.0001), 0.006 (P<0.0001), 0.040 (P<0.001) respectively.

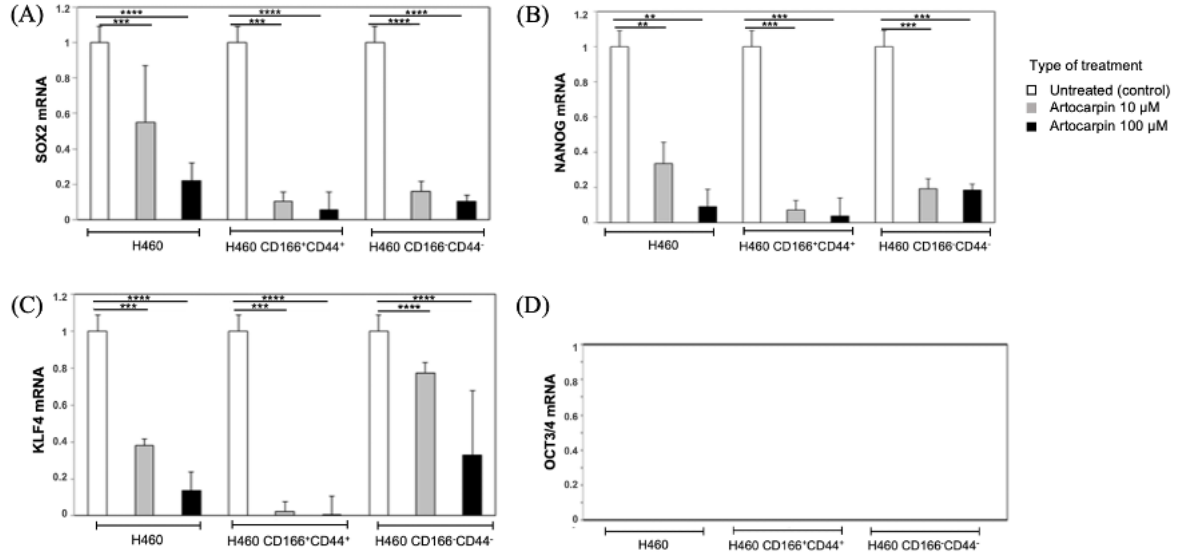

Figure 2. Analyses of the expression of stem cell-related genes in various H460 cell lines. Detectable levels of gene expression (A) SOX2, (B) NANOG and (C) KLF4 were found in all putative CSCs except (D) OCT 3/4. All detectectable mRNA levels in cell lines are expressed as fold change. The negative control was a PCR reaction without a template. Data from three independent cell passages is given as mean ± Standard Error Mean (n=3). One Way ANOVA was used to compare between respective control group. * P <0.05, **P <0.01, *** P <0.001, **** P <0.0001.

3.4. Docking analysis with β-Catenin

The interaction specificities of the artocarpin with β-Catenin were thoroughly examined during the docking study. According to the results obtained, artocarpin formed the best-docked complexes (-7.04 kcal/mol) when compared to the binding energies displayed by known inhibitors such as isorhamnetin, fisetin, genistein, and silibinin (-5.68 to -4.98 kcal/mol), followed by other inhibitors such as catechin, luteolin, coumestrol, and β-naphthoflavone (-6.50 to -5.22 kcal/mol) (Iftikhar and Rashid, 2014). Throughout the test, artocarpin was found to inhibit the binding of β-Catenin. Hydrophobic and hydrogen bonding interactions of docked molecules were compared using the LigPlot program. In any case, Lys345, Val346, and Asn387 residues of β-Catenin were discovered to interact with hydrogen binding. Artocarpin interacted with β-Catenin to form H-bonds in the TCF-interactive region involving residues Glu24, Gln27, Glu29, and Gly25 at distances 2.76893 Å, 2.86867 Å, 2.64498 Å, and 3.74859 Å, respectively. Trp383 formed pi-pi interactions with artocarpin at 4.34458 Å, 4.27395 Å, 5.03811 Å, and 5.02537 Å, respectively. Arg386 formed pi-cation interaction with artocarpin at 3.94659 Å. Meanwhile, artocarpin formed pi-cation interaction with Trp383 at 4.43971 Å, 4.87218 Å, 3.94334 Å, 4.94015 Å, 4.98735 Å, and 4.54912 Å, respectively. Arg386 formed pi-donor H-bond with artocarpin at 3.94659 Å, and Lys345 formed pi-donor H-bond with β-Catenin at 4.0286 Å, respectively.

β-Catenin residues Trp383 and Cys419 were found to be involved with hydrophobic interactions (Figure 3). The interaction of artocarpin with β-Catenin and TCF-4 involved a H-bond acceptor, a H-bond donor, and an aromatic ring. The inhibitory effect of artocarpin that targeting β-Catenin in the Wnt signaling pathway correlates with known inhibitors as they tend to occupy the same binding cavity (Figure 4).

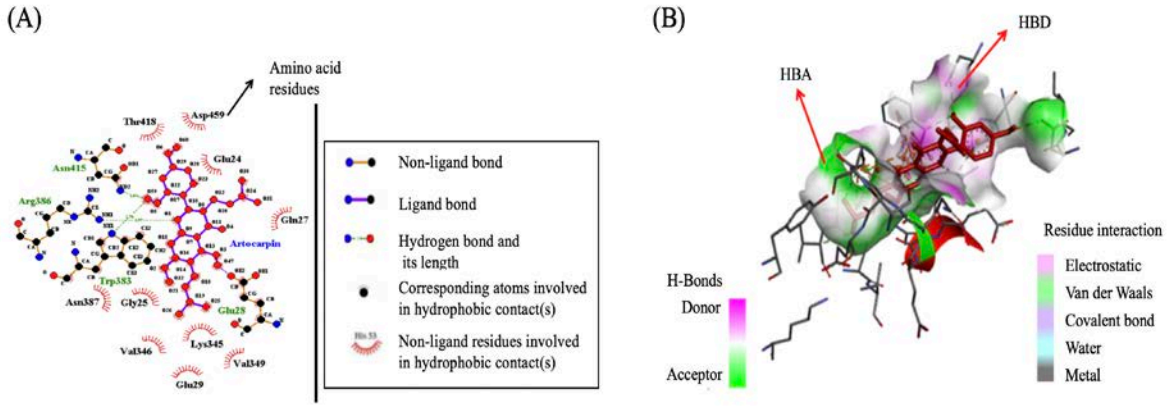

Figure 3. (A) The interacting residues of β-Catenin with the potential inhibitor artocarpin using LigPlot+ (B) Analysis of ligand with β-Catenin active site residue interactions using Discovery Studio Visualizer 4.1 Client.

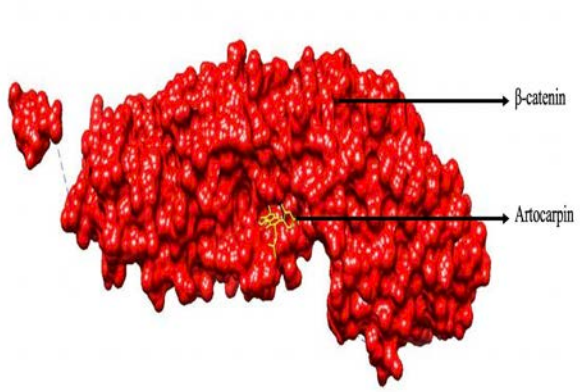

Figure 4. Multiple Ligand Simultaneous Docking (MLSD) Analysis and Molecular Interaction of Artocarpin (shown in yellow) at the Binding Site of β-Catenin. The β-Catenin/Artocarpin complex structure were generated in PyMOL version 2.1.1 (https://pymol.org)

3.5. Docking analysis with WNT

The interaction between artocarpin with WNT protein resulted in the highest binding energy values (-14.91 kcal/mol) compared to other WNT/β-Catenin inhibitors. This result supports the inhibitory activity of artocarpin on lung CSCs with low WNT and β-Catenin gene expression levels. In contrast to the results obtained in this study, Ser120: OG residue of WNT1 was the only one that interacted with hydrogen binding at a distance of 3.76146 Å compared to β-Catenin. Nevertheless, artocarpin and WNT1 formed a hydrophobic interaction that involved many residues, including Pro130, Cys77, Cys122, Pro132, and Leu144, at distance 4.15022 Å (C4); 3.45597 Å; 4.54061 Å, 5.21859 Å for Pro130, 5.11105 Å (C60) for Cys77, 4.05568 Å (C60) and 3.70246 Å (C5) for Cys122, 3.5248 Å (C30) and 3.45622 Å (C31) for Pro132, 4.06423 Å (C26) and 4.71292 Å (C25) for Leu144, respectively. Artocarpin was also interacted with itself to form hydrophobic interaction at a distance 3.40135 Å (C59) and 3.15232 Å (C31). Meanwhile, WNT1 residue (Thr143: CG2) interacted with artocarpin to form hydrophobic interaction at a distance of 3.75129 Å. Other types of interaction were between Cys122: SG residue of WNT1 with artocarpin at a distance of 5.86659 Å and 3.42835 Å (Figure 5).

Ser120: OG formed pi-donor with artocarpin, whereby H-Donor of Ser120: OG interacted with pi-orbitals of artocarpin through this molecular inhibition study. Thr143: CG2 and artocarpin itself (C59 and C31) formed pi-sigma with artocarpin, whereby C-H of Thr143: CG2 and two residues of artocarpin have the interaction with pi-orbitals of artocarpin. WNT1 residue (Cys 122: SG) formed two pi-sulfur interactions with artocarpin, whereby a sulfur group of two residues of Cys122: SG have the interaction with pi-orbitals of artocarpin. Three types of artocarpin residues formed pi-alkyl interaction with Pro130, whereby pi-orbitals of artocarpin have the interaction with the alkyl group of Pro130. Artocarpin residues formed alkyl have the interaction with Pro130 at C4, Cys77 at C60, Cys122 at C60 and C5, Pro132 at C30 and C31, Leu144 at C26 and C25 (Figure 5). The models or figures were evaluated using the PyMOL program (Figure 6).

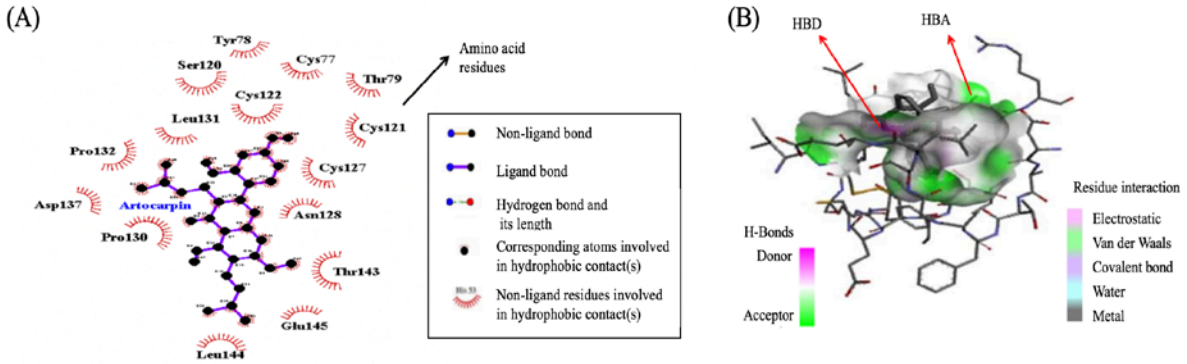

Figure 5. (A) The interacting residues of WNT with the potential inhibitor artocarpin using LigPlot+ (B) Analysis of ligand with WNT active site residue interactions using Discovery Studio Visualizer 4.1 Client.

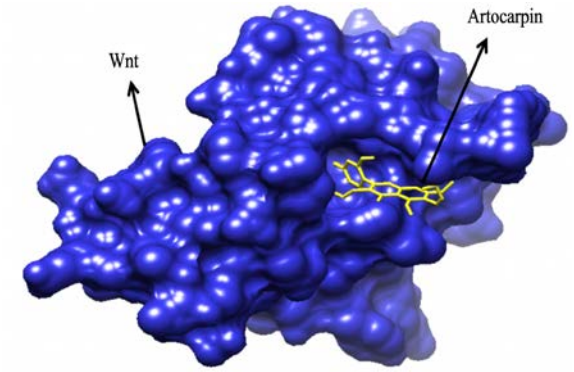

Figure 6. Multiple Ligand Simultaneous Docking (MLSD) Analysis and Molecular Interaction of Artocarpin (shown in yellow) at the Binding Site of WNT. The WNT-Artocarpin complex structure were generated in PyMOL version 2.1.1 (https://pymol.org)

3.6. β-Catenin and WNT expression knockdown

As depicted in Figure 7, artocarpin treatment significantly reduced the expression of both targeted genes; β-Catenin (DACT3) and WNT in all examined cell lines as compared to their respective untreated cell lines. In the artocarpin treated (10 µM and 100 µM) H460 cell lines, the expression of β-Catenin gene was significantly down-regulated with FC value of 0.400, (P<0.01) and 0.1920, (P<0.001) respective to the untreated cells. Similar pattern of inhibition was observed in artocarpin treated lung CSCs $CD166^{+}CD44^{+}$ cells (FC values of 0.400, (P<0.001) and 0.192, (P<0.001) and non-CSCs $CD166^{-}$ CD44 cells (FC value of 0.419, (P<0.01) and 0.339, (P<0.001) respectively for 10 µM and 100 µM artocarpin concentration (Figure 7). Compared to the other two types of cell lines, prominent inhibition was observed in lung CSCs $CD166^{+}CD44^{+}$ cells.

In the expression of WNT gene, similar result was observed in which artocarpin treatment at the dose of 10 µM and 100 µM significantly inhibited its expression in all three examined cell lines compared to their respective untreated groups. The fold change expression for 10 µM and 100 µM artocarpin-treated H460 cells were 0.449 (P <0.01) and 0.387 (P <0.001), meanwhile in lung CSCs $CD166^{+}CD44^{+}$, the result were 0.155 (P<0.05) and 0.078 (P <0.001) and in non-CSCs $CD166^{-}CD44^{-}$, the value were 0.275 (P <0.01) and 0.251(P <0.001), respectively. Based on the readings, artocarpin exerted obvious inhibition in lung CSCs $CD166^{+}CD44^{+}$ compared to the other cell lines similar to β-Catenin (DACT3) gene expression.

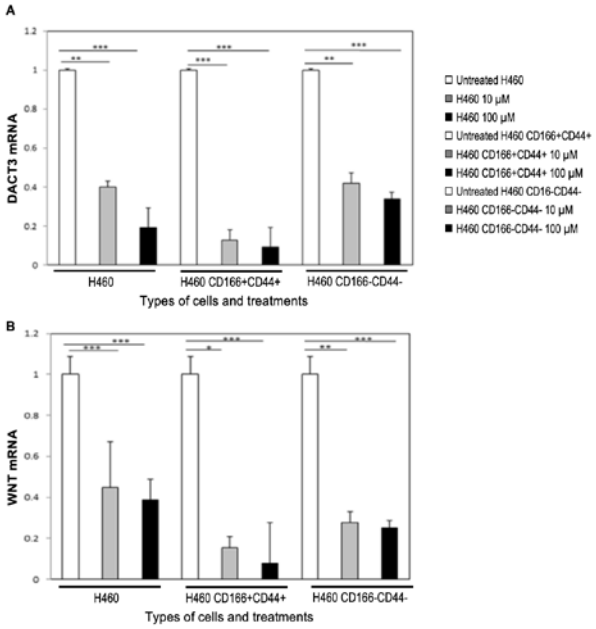

Figure 7. Analysis of targeted genes expression in different cell lines; A) β-catenin (DACT3) and B) WNT. The negative control was the PCR reaction without template. The β-catenin (DACT3) and WNT mRNA levels in cell lines were expressed as mean ± Standard Error Mean (n=3) of fold change from three independent cell passages. Significant *P* value was calculated using the ANOVA test by comparing the treatment groups with the respective untreated group. * P <0.05, **P <0.01, *** P <0.001.

4. Discussion

CSCs, by nature, are the subpopulation of tumour cells responsible for tumour initiation and relapse. Research revealed several regulatory pathways involved in maintaining their self-renewal and differentiation capabilities. Knowing that they own specific biomarkers, targeting this subpopulation and their regulatory signalling has become a promising cancer therapeutic strategy.

Up to the present, neither the scientific data on the isolation of $CD166^{+}CD44^{+}$ CSCs from H460 cell lines nor the effect of artocarpin on these isolated cells has been reported. As a result, this research adds to the pool of data available. In line with the aim of specific targeting, isolation of the CSCs according to their biomarkers in conventional cancer cell lines is one of the fundamental research steps. Several techniques were documented. According to a previous report, several CSC markers were

identified in the lung, such as CD166, CD133, CD44, CD24, ABCG2, ALDH1A1, and EpCAM (Phiboonchaiyanan *et al.,* 2016; Muraro *et al.,* 2012). Therefore, this study was conducted to determine the specific surface biomarkers expressed in isolated CSCs from the H460 lineage using the FACS technique. The results of the flow cytometry analysis in this study supported the hypothesis that the CSCs comprise a heterogeneous population by demonstrating the presence of several phenotypes ($CD166^+CD44^+$, $CD166^-CD44^-$). This finding was aligned with those reported previously in which CD44 and CD166 were detected in parental H460 cancer cell lines (Eun *et al.,* 2017). In this study, the obtained double-positive cells ($CD166^+CD44^+$) were regarded as lung CSCs, meanwhile double-negative cells ($CD166^-CD44^-$) were regarded as non-CSCs. The detection of CD166 and CD44 in this H460 cell line showed that their expressions were the most prominent compared to other CSCs markers. Even though elevated levels of EpCAM expression in many types of cancer demonstrated tumour advancement and malignancy, its levels of expression can be up or downregulated in a certain condition (Mohtar et al., 2020). EpCAM exert potential biphasic influence on the regulation of Epithelial-Mesenchymal Transition (EMT). This multifaceted phenomenon suggests that EpCAM can either augment or mitigate the EMT process in which EpCAM expression is downregulated when cancer cells are in the midst of an EMT event. Within breast and lung cancer cells, there is observable evidence of a transient diminishment in EpCAM expression concurrent with the cells' engagement in EMT during the metastatic progression (Hyun et al., 2016). As has been shown by the result obtained in this study, it is stipulated that the absent of the EpCAM expression in this CSCs population is due to the origin of the cells which is from the pleural effusion which indicates the metastatic characteristic and represent the loss of adhesive properties as it is shed from the primary origin. It is also reported that EpCAM expression is often reduced in certain types of NSCLC (Gastl *et al*., 2000).

Two markers' co-expression was examined to establish a more robust phenotype for the potential CSC population. The previous investigation with a single marker expression revealed that CD166 and CD44 were dominant markers in H460 cell lines, so we investigated CD166 co-expression with CD44 for further sorting in H460 cell lines. The H460 cell line was chosen to be investigated further in this study because the cells express easily detectable p53 mRNA at levels compared to other cells. Figure 1B shows that 62.5% of the H460 cells were $CD166^+CD44^+$ in this isolation process. The H460 cell line's $CD166^+CD44^+$ cells have been sorted and designated as the population of lung CSCs. To confirm the stemness characteristics of the lung CSCs, the $CD166^-CD44^-$ was also isolated where these cells were identified as a non-CSC population with the percentage of expression as 37.5% cells.

As the antiproliferative activity of a compound towards cellular growth is suggestive of its anticancer properties, a toxicity study of artocarpin on parental H460 cell line was performed, and the result positively reflected our hypothesis. In determining the capability of artocarpin in targeting the isolated subpopulation of CSCs in the H460 cell line, the MTT assay was carried out. The reduction in the number of living cells of H460 CSCs observed upon artocarpin treatment indicates that artocarpin acts as an effective H460 CSCs cytotoxic compound, incidating that this compound inhibits lung CSCs. A strong cytotoxic activity against this subpopulation proposed the specific supression of this compound on the CSCs, thus postulating the possible targeted inhibition of artocarpin to cancer progression. This data further supports the previous evidence that artocarpin has anticancer effects due to its chemical structure, which includes C-3 prenylated flavones that contribute to the compound's cytotoxic effects thus suggesting it as a potential anticancer agent (Satar et al., 2018).

In the context of pluripotency, certain transcription factors play a pivotal role in maintaining tumour heterogeneity. To further evaluate the anti-cancer mechanism exerted by artocarpin towards the CSCs, the study on the pluripotency-associated markers such as NANOG, SOX2, KLF4 and OCT3/4 was conducted in all H460 cell lineages. The result revealed that artocarpin attenuated the expression of examined genes except OCT3/4. NANOG is correlatively expressed in many CSCs, especially in $CD133^+$ and $CD44^+$ cancer cells. The involvement of NANOG in embryonic development and cellular reprogramming validates their significant contribution to disease prognosis (Mahalaxmi *et al.,* 2019).

Further evidence supports that dysregulation of SOX2 induces resistance toward cell death and chemotherapy as this gene initiates the cell cycle (Hüser *et al.,* 2018). Along with the role of SOX2, NANOG, and c-MYC in generating an induced pluripotent cell, KLF4 helps reprogram the somatic cell into its pluripotent state and maintenance. In addition, KLF4 was found to be associated with Epithelial-Mesenchymal Transition (EMT) that implicated cancer metastasis (Zhou *et al.,* 2022). The OCT3/4, also known as POU5F1, is a transcription factor essential for developing pluripotent stem cells. It is expressed in embryonic stem cells, germ cells, and some cancer cells (Torres-Padilla & Chambers, 2014). The unexpressed level of OCT3/4 in our studied lung CSC was supported by previous findings in which this gene was undetected in H460 cell lineage using variety of detection techniques, including as immunohistochemistry, Western blotting, and RT-PCR. Another possible explanation for this finding includes the state of the cell itself in which H460 cells are more differentiated than the embryonic stem and germ cells, and yet they undergo changes in gene expression profile. Besides, there was possible mutation or alteration in the gene's regulatory regions and complex machinery that led to its downregulation, expression, or silencing (Yang *et al.,* 2011). The lack of detection of the OCT 3/4 gene in this study is consistent with previous data on the presence or absence of OCT 3/4 genes in a variety of cell lines, including distal oesophageal adenocarcinoma (ESO51), cervical cancer cell line (HeLa), lung adenocarcinoma (H460), and colorectal adenocarcinoma (H716B) (Rijlaarsdam *et al.,* 2011). As this compound significantly attenuates the expression level of the dominant oncogene, it brings hope to a novel therapeutic target for CSC elimination.

As artocarpin can inhibit the activity of CSCs development (Nonpanya *et al.,* 2021); it is worthwhile to identify the mechanistic action of this potential anticancer agent. In order to investigate the effect of artocarpin against the WNT/β-Catenin pathway, the preliminary

investigation was done through the molecular docking process of both WNT and β-Catenin protein with artocarpin and validated with gene expression assay of WNT and β-Catenin mRNA levels of the treated isolated CSCs. These methods provided useful preliminary evidence to support the selection of a suitable target for treating lung CSCs via the WNT/β-Catenin pathway.

Up to current research, many flavonoids, a family of naturally occurring compounds, have been found to mediate their regulatory activity towards a variety of cellular targets using a WNT/β-Catenin pathway. WNT/β-Catenin inhibitors, including fisetin, apigenin, isorhamnetin, silibinin, genistein, catechin, luteolin, coumestrol, and β-napthoflavone are well-known to suppress WNT/β-Catenin complex activation (Sferrazza *et al*., 2020). As artocarpin is a member of the flavonoid and capable of attenuating the CSC activities, the possible interaction of this compound with WNT and β-Catenin was further studied. The molecular docking of this compound against the WNT/β-Catenin complex was performed to screen the binding site details. Molecular docking is a computational method that is used to predict the interactions between two molecules. In the context of the WNT/β-Catenin signaling pathway, molecular docking can be used to predict the interactions between artocarpin with the WNT and β-Catenin proteins. Compared to the other flavonoids, artocarpin was shown to form a best-dock complex with both proteins.

In this study, artocarpin molecule binds to its respective targets (β-Catenin and WNT protein) with a high affinity. Docking studies of prenyl flavone artocarpin at the bioactive sites of β-Catenin and WNT indicated that 3D structural folding at the protein-ligand groove is a distinguishing feature for molecular recognition of targeted chemicals and predicting their biological function. Artocarpin interacted with TCF-4/β-Catenin through an H-bond acceptor, an H-bond donor, and an aromatic ring. This means that artocarpin is likely to bind to the complex binding site. A similar interaction trend in terms of binding energy and region on targeted WNT/β-Catenin complex makes artocarpin comparable to other known inhibitors. The findings also showed that hydrogen bonding and hydrophobic interactions maintained the ligands at the target site, influencing binding affinity and therapeutic efficacy. In this molecular docking study, it is postulated that artocarpin binds to the WNT and β-Catenin proteins, thus inhibiting the interaction of the protein with the other complex molecules.

Behind the expression of stemness, angiogenesis, and cell cycle regulator's gene in cancer homeostasis, transcription factors act as drivers in this signalling, which includes TCF/LEF (Moon *et al.*, 2008), FOX (Ito & van den Heuvel, 2011) and SOX family (Zhang & Wang, 2014). In lung CSCs, the WNT/β-Catenin pathway is often dysregulated, thus leading to the overexpression of transcription factors such as TCF7L2 that promote CSC growth and survival (Zhang *et al.*, 2015). T-cell factor 4 (TCF-4), the family of TCF/LEF, is the master player of the canonical WNT signalling pathway. In response to the activation of the pathway by binding of the WNT ligand to its receptor, accumulated β-Catenin will interact with TCF-4, forming β-Catenin/TCF-4 complex. The binding of this complex molecule had switched the role of TCF-4 from repressor to the activator of gene expression. The DNA-binding domain on this molecule allows the complex to bind to the specific DNA target, known as WNT response elements (WREs), and subsequently undergoes gene transcription (Wang *et al.*, 2018).

Regarding the knowledge of this signalling, inhibition of any component in the signalling, especially the β-Catenin and TCF-4, may inhibit progressive cell proliferation and thus inhibit the proliferation of cancer cells (Lu *et al*., 2014). Previous structural and biochemical studies showed that the central portion of the TCF/β-Catenin binding domain is required for TCF to be anchored to β-Catenin via two conserved lysines in β-Catenin (Anthony *et al.* 2020). Liu and his team stated that TCF proteins act as a transcriptional enhancer by binding with an enzyme known as histone methyltransferase (HMT) (Liu *et al*., 2015). As the core of TCF-4 binding residues in the β-Catenin active site pocket was pre-loaded with an inhibitor, transcription of the target genes would be prevented. The interaction of artocarpin with TCF-4/β-Catenin complex with crystal structure showed that this compound occupied a similar inhibitory mechanism. From molecular docking analysis, it is stipulated that artocarpin attenuates the stemness gene expression by intercepting the interaction of β-Catenin to this molecule, thus preventing the TCF-4/β-Catenin complex formation and subsequent gene expression.

This result further supports the previous findings on the anticancer activity of this compound on various cancer cell lines, including human leukaemia HL-60 (CCL-240) cells, colorectal adenocarcinoma HT-29 (HTB38) cells, breast adenocarcinoma cancer MCF-7 (HTB-22) cell, and non-small lung cancer H460 (HTB-177) cell lines (Daud *et al.*, 2019; Mat Daud *et al*., 2021). Furthermore, in H460, artocarpin displayed antiproliferation, antidifferentiation, antimigration, and anti-invasion capabilities (Daud *et al.*, 2020). Though molecular docking analysis is useful in predicting the interaction between molecules and identifying potential therapeutic agents, confirmatory analysis is a must. The expression of DACT3, a member of the DACT (Drp/Frodo) gene family WNT/β-Catenin genes upon treatment with this compound, was further evaluated to determine the reliability of the docking simulation. The ability of artocarpin to reduce the DACT3 gene expression determines the direct inhibition of this compound on this signalling pathway. Reduction in nuclear β-Catenin prevents the direct formation of the TCF-4/β-Catenin complex, thus down-regulating the subsequent mechanism (He *et al*., 2014). Unlike other WNT signalling inhibitors, which suppressed DNA methylation, DACT3 repression was linked to bivalent histone modification. Both histone methylation and deacetylation strongly inhibit Dishevelled (Dvl)-mediated WNT/β-Catenin signalling, resulting in cancer cell death (Trejo-Solis *et al*., 2021). The result clarifies the specific mechanism artocarpin exerts in suppressing the growth and stemness characteristic of lung CSCs. All these shreds of evidence and the current findings supported the involvement of intracellular signalling cascade by artocarpin to ameliorate several detrimental occasions in the onset of cancer relapses. Participation of this compound by binding to the respective proteins down to the modulation of oncogene expression makes artocarpin on par with the other anticancer candidates. Resolution of the WNT/β-Catenin degradation

pathway by artocarpin greatly enhanced the current understanding of the biological roles of artocarpin and the diverse functions of transcription factors as such WNT signalling intermediates or target genes in the normal and disease state.

These data provide valuable insights of artocarpin and its anticancer activity. However, it is important to acknowledge the limitations inherent in this research. Despite the most expressed and studied surface marker detected in H460 cell lines, another possible marker could be evaluated, such as ALDH1, which is believed to be expressed at a low level in certain cancer stem cells as being recently published (Wei *et al*., 2022). As ALDH1 is responsible for producing an enzyme that is crucial for cellular processes, and its overexpression was observed in certain types of cancer, it is worthwhile to investigate the presence of this molecule in H460 cell lines and thus evaluate the interaction of artocarpin on this molecule in the future study.

These overall findings provide a conceptual framework for the protective effect of artocarpin on these cell lines against metastasis and cancer resistance. These molecular mechanisms may be harnessed to develop drugs that help prevent and treat the impairment of abnormal cell division. The study has shed light on developing an envisaged therapeutic strategy using the active compounds from plant-based natural products against cancer resistance in lung cancer. Overall, it is believed that a better understanding of the mechanisms underlying the anticancer properties of artocarpin and its attributive roles would facilitate the development of promising lung cancer therapeutics using herbal medicine.

5. Conclusion

As CSCs are at the core of cancer treatment failure, targeting this subpopulation has been shown to be a promising treatment strategy. This study established the possibility of isolating the CSCs from the lung's H460 cell line and proved the artocarpin capability to inhibit the stemness characteristic of this subpopulation. With the aid of molecular docking, screening this compound's binding activity towards the specific component of the cancer signalling pathway helps understand its anticancer activities. However, further research is required into the suggested inhibitor, particularly its binding and inhibitory potential *in vivo*. This data has yet to generate a pharmacophore model with common pharmacophoric features. It can be used to screen more compounds, which will aid in discovering novel inhibitors of β-Catenin and, hence, the WNT signalling activation pathway in lung cancer.

Acknowledgements

This laboratory works is funded by the Ministry of Higher Education Malaysia (FGRS/1/2017/SKK06/UNISZA/03/1(RR237)). Special thanks go to Universiti Sultan Zainal Abidin for assisting in developing and evaluating the proposed framework and providing funds for publication. Appreciation also goes to Universiti Sains Malaysia, Kepala Batas, and all the lab staff for facilitating this molecular research and sharing their expertise.

References

Abd Wahab NZ and Ibrahim N. 2022. Styrylpyrone Derivative (SPD) Extracted from Goniothalamus umbrosus Binds to Dengue Virus Serotype-2 Envelope Protein and Inhibits Early Stage of Virus Replication. *Molecules*, **27(14)**:4566.

Almajali B, Al-Jamal H, Taib W, Ismail I, Johan MF, Doolaanea AA and Ibrahim WN. 2021. Thymoquinone, as a Novel Therapeutic Candidate of Cancers. *Pharmaceuticals*, **14(4)**:369.

Anthony CC, Robbins DJ, Ahmed Y and Lee E. 2020. Nuclear regulation of Wnt/β-catenin signaling: It'sa complex situation. *Genes*, **11(8)**:886.

Chen HY, Bohlen JF and Maher BJ. 2021. Molecular and Cellular Function of Transcription Factor 4 in Pitt-Hopkins Syndrome. *Dev Neurosci*. **43(3-4)**:159-167.

Daud NN, Septama AW, Simbak N, Rahmi EP. 2020. The phytochemical and pharmacological properties of artocarpin from Artocarpus heterophyllus. 2020. *Asian Pac J Trop Med.*,**1;13(1)**:1-7.

Daud NN, Septama AW, Simbak N, Bakar NH, Rahmi EP 2019. Synergistic Effect of Flavonoids from Artocarpus heterophyllus Heartwoods on Anticancer Activity of Cisplatin Against H460 and MCF-7 Cell Lines. 2019. *Nat. Prod. Sci.,* **1;25(4):**311-6.

Eun K, Ham SW and Kim H. 2017. Cancer stem cell heterogeneity: origin and new perspectives on CSC targeting. *BMB Rep.,* **50(3)**:117.

Fleige S, Walf V, Huch S, Prgomet C, Sehm J and Pfaffl MW. 2006. Comparison of relative mRNA quantification models and the impact of RNA integrity in quantitative real-time RT-PCR. *Biotechnol Lett.*, **28**:1601-13.

Forrest MP, Hill MJ, Quantock AJ, Martin-Rendon E and Blake DJ. 2014. The emerging roles of TCF4 in disease and development. *Trends Mol Med.*, **20(6)**:322-331.

Gastl G, Gunsilius E, Beug H, v. Schweinitz D. 2000. Epithelial cell adhesion molecule expression in non-small cell lung cancer (NSCLC). *Lung Cancer*, **29(3)**: 215-221.

Hassan M, Baig AA, Attique SA, Abbas S, Khan F, Zahid S, Ain QU, Usman M, Simbak NB, Kamal MA and Yusof HA. 2021. Molecular docking of alpha-enolase to elucidate the promising candidates against Streptococcus pneumoniae infection. *Daru.*, **29**:73-84.

He QZ, Luo XZ, Wang K, Zhou Q, Ao H, Yang Y, Li SX, Li Y, Zhu HT and Duan T. 2014. Isolation and characterization of cancer stem cells from high-grade serous ovarian carcinomas. *Cell Physiol Biochem.*, **33(1)**:173-84.

Huang T, Song X, Xu D, Tiek D, Goenka A, Wu B, Sastry N, Hu B and Cheng SY. 2020. Stem cell programs in cancer initiation, progression, and therapy resistance. *Theranostics*, **10(19)**:8721-8743.

Hüser L, Novak D, Umansky V, Altevogt P and Utikal J. 2018. Targeting SOX2 in anticancer therapy. *Expert Opin Ther Targets.*, **22(12)**:983-91.

Hwang JS, Yoon CK, Hyon JY, Chung TY and Shin YJ. 2020. Transcription Factor 4 Regulates the Regeneration of Corneal Endothelial Cells. *Invest Ophthalmol Vis Sci.*, **61(4)**, 21.

Hyun, Kyung-A., Gi-Bang Koo, Hyunju Han, Joohyuk Sohn, Wonshik Choi, Seung-Il Kim, Hyo-Il Jung, and You-Sun Kim. 2016. Epithelial-to-mesenchymal transition leads to loss of EpCAM and different physical properties in circulating tumor cells from metastatic breast cancer. *Oncotarget.*, **7(17)**: 24677.

Iftikhar H and Rashid S. 2014. Molecular docking studies of flavonoids for their inhibition pattern against β-catenin and pharmacophore model generation from experimentally known flavonoids to fabricate more potent inhibitors for Wnt signaling pathway. *Pharmacogn Mag.*, **10(Suppl 2)**:S264.

Ito T and van den Heuvel MJ. 2011. FOX transcription factors in Wnt signaling. *Curr Opin Cell Biol.*, **23(5)**: 584-591.

Jahanafrooz Z, Mosafer J, Akbari M, Hashemzaei M, Mokhtarzadeh A and Baradaran B. 2020. Colon cancer therapy by focusing on colon cancer stem cells and their tumour microenvironment. *J Cell Physiol.*, **235(5)**:4153-4166.

Khatami, F., Aghaii, M. and Tehrani, F.D., 2020. Cancer stem cells. **Stem Cells in Urology**, pp.15-34.

Liu RL, Dong Y, Deng YZ, Wang WJ and Li WD. 2015. Tumor suppressor miR-145 reverses drug resistance by directly targeting DNA damage-related gene RAD18 in colorectal cancer. *Tumour Biol*., **36 (7)**: 5011-5019.

Lu FI, Sun YH, Wei CY, Thisse C and Thisse B. 2014. Tissue-specific depression of TCF/LEF controls the activity of the Wnt/β-catenin pathway. *Nat Commun.*, **5(1)**:5368.

Mahalaxmi I, Devi SM, Kaavya J, Arul N, Balachandar V and Santhy KS. 2019. New insight into NANOG: A novel therapeutic target for ovarian cancer (OC). *Eur J Pharmacol.*, **852**:51-7.

Makena MR, Ranjan A, Thirumala V and Reddy AP. 2020. Cancer stem cells: Road to therapeutic resistance and strategies to overcome resistance. *Biochim Biophys Acta Mol Basis Dis.*, **1866(4)**:165339.

Masciale V, Grisendi G, Banchelli F, D'Amico R, Maiorana A, Sighinolfi P, Stefani A, Morandi U, Dominici M and Aramini B. 2019. Isolation and identification of cancer stem-like cells in adenocarcinoma and squamous cell carcinoma of the lung: a pilot study. *Front Oncol.*, **9**:1394.

Mat Daud NN, Abu Bakar NA, Septama AW. 2021. In Vitro Anti-proliferative Properties of Flavonoids Isolated from Artocarpus Heterophyllus on Cancer Cell Lines. *Nat Prod J.*, **1;11(5):**755-61.

Mohtar MA, Syafruddin SE, Nasir SN, Low TY. 2020. Revisiting the roles of pro-metastatic EpCAM in cancer. *Biomolecules*. **7;10(2)**:255.

Muraro MG, Mele V, Däster S, Han J, Heberer M, Cesare Spagnoli G and Iezzi G. 2012. $CD133^+$, $CD166^+$ $CD44^+$, and $CD24^+$ $CD44^+$ phenotypes fail to reliably identify cell populations with cancer stem cell functional features in established human colorectal cancer cell lines. *Stem Cells Transl Med.*, **1(8)**:592-603.

Moon RT and Glass CK. 2008. TCF/LEF transcription factors: key regulators of Wnt signaling. *Genes Dev.*, **22(20)**: 2785-2810.

Nimmakayala RK, Batra SK, Ponnusamy MP. 2019. Unraveling the journey of cancer stem cells from origin to metastasis. *Biochim Biophys Acta Rev Cancer*., **1871(1)**:50-63.

Nonpanya N, Sanookpan K, Sriratanasak N, Vinayanuwattikun C, Wichadakul D, Sritularak B and Chanvorachote P. 2021. Artocarpin Targets Focal Adhesion Kinase-Dependent Epithelial to Mesenchymal Transition and Suppresses Migratory-Associated Integrins in Lung Cancer Cells. *Pharmaceutics*, **13(4)**:554.

Phiboonchaiyanan PP, Kiratipaiboon C, Chanvorachote P. 2016. Ciprofloxacin mediates cancer stem cell phenotypes in lung cancer cells through caveolin-1-dependent mechanism. *Chem Biol Interact.*, **250**: 1–11.

Pouremamali F, Vahedian V, Hassani N, Mirzaei S, Pouremamali A., Kazemzadeh H and Maroufi NF. 2022. The role of SOX family in cancer stem cell maintenance: With a focus on SOX2. *Pathol Res Pract.*, **153783**.

Rijlaarsdam MA, Van Herk HA, Gillis AJ, Stoop H, Jenster G, Martens J, Van Leenders GJ, Dinjens W, Hoogland AM, Timmermans M and Looijenga LH. 2011. Specific detection of OCT3/4 isoform A/B/B1 expression in solid (germ cell) tumours and cell lines: confirmation of OCT3/4 specificity for germ cell tumours. *Br J Cancer.*, **105(6)**:854-63.

Satar NA, Fakiruddin KS, Lim MN, Mok PL, Zakaria N, Fakharuzi NA, Abd Rahman AZ, Zakaria Z, Yahaya BH and Baharuddin P. 2018. Novel triple-positive markers identified in human non-small cell lung cancer cell line with chemotherapy-resistant and putative cancer stem cell characteristics. *Oncol Rep*., **40(2)**:669-81.

Septama AW and Panichayupakaranant P. 2015. Antibacterial assay-guided isolation of active compounds from Artocarpus heterophyllus heartwoods. *Pharm Biol.*, **53(11)**:1608-13.

Sferrazza G, Corti M, Brusotti G, Pierimarchi P, Temporini C, Serafino A and Calleri E. 2020. Nature-derived compounds modulating Wnt/β-catenin pathway: A preventive and therapeutic opportunity in neoplastic diseases. *Acta Pharm Sin B.*, **10(10)**:1814-34.

Torres-Padilla ME, Chambers I. 2014. Transcription factor heterogeneity in pluripotent stem cells: a stochastic advantage. *Development*, **141(11)**:2173-81.

Trejo-Solis C, Escamilla-Ramirez A, Jimenez-Farfan D, Castillo-Rodriguez RA, Flores-Najera A and Cruz-Salgado A. 2021. Crosstalk of the Wnt/β-catenin signaling pathway in the induction of apoptosis on cancer cells. *Pharmaceuticals*, **14(9)**:871.

Van Schaijik B, Davis PF, Wickremesekera AC, Tan ST and Itinteang T. 2018. Subcellular localisation of the stem cell markers OCT4, SOX2, NANOG, KLF4 and c-MYC in cancer: a review. *J Clin Pathol.*, **71(1)**: 88-91.

Wang J, Chen J and Chen J. 2018. The WNT signaling pathway in cancer. *Cancer Biol. Ther.*, **19(2)**: 217-228.

Wei Y, Li Y, Chen Y, Liu P, Huang S, Zhang Y, Sun Y, Wu Z, Hu M, Wu Q and Wu H. 2022. ALDH1: A potential therapeutic target for cancer stem cells in solid tumors. *Front Oncol*., **12**:1026278.

Yang L, Shi P, Zhao G, Xu J, Peng W and Zhang J. 2020. Targeting cancer stem cell pathways for cancer therapy. *Signal Transduct Target Ther.*, **5**:8.

Zakaria N, Yusoff NM, Zakaria Z, Lim MN, Baharuddin PJ, Fakiruddin KS and Yahaya B. 2015. Human non-small cell lung cancer expresses putative cancer stem cell markers and exhibits the transcriptomic profile of multipotent cells. *BMC cancer*, **15(1)**:1-6.

Zhan T, Rindtorff N and Boutros M. 2017. Wnt signaling in cancer. *Oncogene*, **36**:1461–73.

Zhang X and Wang Y. 2014. SOX transcription factors in Wnt signaling. *J Cell Physiol.*, **229(10)**: 2287-2297.

Zhou H, Guan Q, Hou X, Liu L, Zhou L, Li W and Liu H. 2022. Epithelial-mesenchymal reprogramming by KLF4-regulated Rictor expression contributes to metastasis of non-small cell lung cancer cells. *Int J Biol Sci.*, **18(13)**:4869.